

Sustainable Synthesis of Silver Nanoparticles via *Zinnia Elegans* Leaf Extract: A Nano Catalytic Approach in Catalysis Applications

Gyruke Goonewardene., Mathivathani Kandiah., Beneli Gunaratne., Ominda Perera

School of Science, Business Management School, Colombo 00600, Sri Lanka

DOI: <https://doi.org/10.51584/IJRIAS.2025.10020058>

Received: 11 February 2025; Accepted: 18 February 2025; Published: 24 March 2025

ABSTRACT

The green synthesis of silver nanoparticles (AgNPs) has gained significant attention as an environmentally friendly and sustainable approach to nanomaterial production. This method leverages biological resources, such as plant extracts, which serve as natural reducing and stabilizing agents. This study investigates the synthesis of AgNPs using five different varieties of *Zinnia elegans* leaves (yellow, pink, white, orange, and magenta), highlighting their promising applications in different fields by evaluating the photocatalytic, para-nitrophenol (PNP) catalytic, antibacterial, and cytotoxic qualities. Under optimum conditions, water extracts (WE) and silver nitrate (AgNO_3) were used to synthesize the AgNPs. Using UV-Visible spectroscopy and scanning electron microscopy (SEM), AgNPs were characterized. The results indicated that Magenta_AgNPs are spherical and 30–60 nm. In the presence of sunlight and the addition of sodium borohydride (NaBH_4), the photocatalytic impact of different concentrations of AgNP was assessed using methyl orange (MO). Upon addition of NaBH_4 , 4000 ppm Magenta_AgNP demonstrated a rapid rate of degeneration. PNP degradation was used to assess the catalytic properties of AgNPs. All AgNP demonstrated PNP degradation, with Pink_AgNP exhibiting the highest degradation rate. *Escherichia coli* and *Staphylococcus aureus* were used to determine the antibacterial activity of AgNPs and WEs; only AgNPs produced a zone of inhibition (ZOI). An AgNP cytotoxicity study was conducted with *Artemia salina*, which demonstrated 100% viability at concentrations of 800 ppm and 240 ppm. The findings highlight that AgNPs synthesized using *Zinnia elegans* hold considerable promise for advancing eco-friendly approaches in environmental remediation and antibacterial therapy, offering a platform for future applications.

Keywords: Silver nanoparticle; *Zinnia elegans*, photocatalysis, methyl orange, para-nitrophenol, antibacterial, cytotoxicity

INTRODUCTION

Sri Lanka and India are reported to have a 40% flower yield and also largely contribute to the daily flower wastage [1]. The heavy disposal of these ornamental flowers has contaminated water bodies, and proper separation during disposal is an added problem. The existing disposal method is to incinerate the floral waste, which contributes to air pollution, and dispose of it into open areas, which can lead to environmental problems. The waste contains a high amount of bioactive compounds that can be utilized in several industries, such as food and medicine [2,3]. Efforts to find sustainable solutions for the disposal of floral waste are crucial in order to minimize environmental impacts and maximize the potential benefits of the bioactive compounds present.

Zinnia elegans is one such floral waste that has shown promising bioactive properties, making it a valuable resource for various industries. It belongs to the *Zinnia* genus, which is a member of the Asteraceae family that originated in South America and Mexico. These are well-known for their many properties, including antibacterial, antimalarial, and antioxidant qualities [4,5]. *Zinnia elegans* is classified as an ornamental plant and is widely grown as a garden plant. The blossoms of this plant come in a variety of colors and heights. It has fewer leaves and tiny, solitary blooms. Previous studies have documented the presence of various secondary metabolites such as steroids, saponins, flavonoids, polyphenols, and alkaloids. The presence of these bioactive compounds is attributed to the plant's potential antioxidant, anti-inflammatory, and antimicrobial properties [6,7]. A thorough investigation of *Zinnia* leaf extracts has not yet been carried out and is considered a waste, despite the fact that earlier research has centered on the several uses of this species' flowers due to its ornamental features. This study focuses on exploiting these *Zinnia elegans* leaves beyond their aesthetic value

in the synthesis of nanoparticles, thereby evaluating their diversified potential and helping reduce the waste burden on the environment.

A promising field of study to address the current environmental pollution due to toxic substance leakage into wastewater is the application of nanotechnology as a remediation solution. This has brought attention to the significance of investigating environmentally friendly and sustainable remediation techniques. At the core of nanotechnology are nanoparticles, which are tiny marvels of engineering ranging from 1 to 100 nanometers in size. They possess unique biological, chemical, and physical properties. With their high surface-to-volume ratio, nanoparticles contribute to advancement and innovations in various fields [8].

Nanoparticles can be synthesized using two primary methods: the top-down strategy, which involves energy to break down bigger components to form nanoparticles, and the bottom-up approach, which involves allowing atoms or chemical species to undergo reactions to generate nanoparticles [9]. A top-down approach is performed by the use of physical methods, and a bottom-up approach is performed by the use of chemical or biological methods. Physical and chemical synthesis of nanoparticles are costly, not environmentally friendly, and possess high reagent requirements compared to biological synthesis [10]. The use of plants or microorganisms in the synthesis is an example of biological methods. Plant-mediated synthesis is preferred over microbial-mediated synthesis due to its simplicity, presence of naturally existing phytochemicals, biocompatibility, speed, and scalability [11]. Utilizing these different methods of synthesis, different metal nanoparticles such as gold, copper, silver and zinc can be synthesized. This research utilizes silver over other types of metal due to their cost-effectiveness, better antimicrobial properties, wider versatility, and accessibility for various applications [12]. The unique properties of AgNPs make them ideal for synthesizing and evaluating photocatalytic activity, PNP degradation, cytotoxicity, and antibacterial efficacy.

Currently, many industries release dye effluents without complete degradation. The degradation of these organic contaminants is essential before their release into the environment, as they are associated with splenic sarcomas and human cancers [13]. Azo dyes are one group of commonly used dyes that comprise more than 60% of textile dyes, and about 15 to 20% of these unbound azo dyes contaminate the water bodies. These dyes have a characteristic functional group, $-N=N-$, and an increase in these azo bonds increases the molecular weight of the dye, causing slow degradation [14,15]. The most common azo dyes include methylene blue, methyl red, and MO. MO is carcinogenic, water-soluble, low-biodegradable, and classified as an anionic or acidic dye [16]. Inefficient degradation of these azo dyes before the release into wastewater is proven to cause toxic effects on living organisms and decrease crop quality and soil fertility [17,18]. Conventional methods such as photocatalysis using TiO_2 , biological treatments, and advanced oxidation processes are present, but they are costly and produce harmful byproducts. However, the utilization of AgNPs as an alternative is in high demand. This is due to their ability to become activated by light and produce reactive oxygen species (ROS) that degrade organic contaminants. Due to their abundance of catalytic sites, high stability, and recyclability, AgNPs have been shown to be the most effective substitute for toxic dye degradation [19].

PNP is another hazardous wastewater contaminant that is used in both industrial and agricultural settings. PNP is highly toxic to aquatic life; causes soil contamination and is a risk to human health. Hence, necessary degradation methods must be employed to eradicate it from the environment [20]. PNP can be degraded using conventional methods such as using TiO_2 and chemical oxidation using ozone or H_2O_2 . However, due to the catalytic activity of AgNPs and their high surface-to-volume ratio, they can absorb PNP onto their surfaces efficiently aiding in degradation. The usage of AgNPs is much more eco-friendly and stable compared to the conventional methods [21].

Presently, the available antibiotics have diminished effectiveness in antibacterial effect with time due to the development of antibiotic resistance [22]. This antibacterial effect refers to the capacity of a chemical or substance to eradicate the proliferation of bacteria at a specific location whilst being non-toxic to the surrounding environment [23]. To minimize this issue, conventional methods like the usage of chemicals such as chlorine are present, which are not stable and will lose effectiveness with time [24]. The multidrug-resistant bacterial strains have not been completely eradicated by these current options. With regard to their greater antibacterial efficacy against a wide range of bacteria, AgNPs can be employed either alone or in combination with currently available antibiotics. AgNP's capacity to break down bacterial cell walls and disrupt their

defense mechanisms is thought to be the cause of its antibacterial qualities [25,26]. The effectiveness of AgNP as an antibacterial agent will depend on a number of factors, including its size, shape, and dosage [27].

AgNPs have various uses in several fields, and it is essential to ensure their safety before being used for their applications. AgNPs can induce cytotoxicity by their ability to produce ROS, resulting in oxidative stress to cellular components; hence, it is essential to ensure their safety before being used for their applications [28]. It is crucial to evaluate AgNPs for cytotoxicity because of their discharge into water bodies, oxidation into Ag⁺ ions, and subsequent accumulation in aquatic organisms that will lead to exposure by humans [29,30]. Conventional methods such as the MTT assay, LDH assay, and usage of various model organisms such as fruit flies and zebrafish are present. However, *Artemia salina* (brine shrimp) is used to assess cytotoxicity, as conventional methods often are more time-consuming and require complex equipment. Usage of brine shrimp, on the other hand, is cost-effective and highly sensitive to toxic substances. In the context of ethical considerations, brine shrimp present fewer concerns compared to other model organisms, hence providing freedom in cytotoxic testing [31].

The study aims to explore the potential of *Zinnia* leaf extracts in the synthesis of AgNPs and to investigate its photocatalytic capacity using MO dye, PNP degradation capacity, antibacterial effect against *Escherichia coli* and *Staphylococcus aureus* and cytotoxic effect using *Artemia salina*. AgNP characterization using SEM will be performed. If the aims of the study are, achieved AgNPs produced by *Zinnia* extracts can be used in bioremediation and as antibacterial alternatives.

METHODOLOGY

Sample collection

The *Zinnia* leaves of five species (Fig. 1) used in the study were sourced from Kelaniya, Sri Lanka. They were collected, cleaned, and shade dried for 48 hours.



Fig. 1 Five varieties of *Zinnia elegans* leaves ;(a) Pink, (b) White, (c) Orange, (d) Magenta and (e) Yellow

Water extraction method

The dried leaves were crushed, and 2 g of each sample was added to 50 ml of distilled water (DW) and incubated at 60°C for one hour. The obtained water extracts were filtered using Whatman filter paper no. 1 and were stored in Falcon tubes at 4°C for future use [32].

Synthesis of AgNPs

1 mL of WE was mixed with 9 mL of 1 mM AgNO₃ and incubated at 60 °C and 90 °C for 15, 30, 45 and 60 min and at room temperature (RT) for 24 hours. They were then stored at 4 °C until further use [32].

Characterization of AgNP

Using spectrophotometry

Using the UV-Vis spectrophotometer, the absorbance was recorded for a wavelength range of 320-520nm, with DW serving as the blank solution.

Using SEM

1 mL of 4000ppm Magenta_AgNP was centrifuged at 13,000 rpm for 2 minutes and repeated until a prominent pellet appeared while discarding the supernatant. The pellet was oven dried at 40 °C for 24 hours to remove any remaining liquid. The sample was gold coated using a sputter coater before analysis. The analysis was performed in Sri Lanka Institute of Nanotechnology (SLINTEC) using HITACHI SU6600 SEM.

Determination of the photocatalytic activity of AgNPs in degrading MO

The absorbance of a 1 ppm MO aqueous solution was measured between 350 and 530 nm. 100 mL of MO solution was combined with 1 mL of AgNPs at concentrations of 4000 ppm and 267 ppm in order to evaluate the photocatalytic impact of AgNPs. Absorbance was measured every 15 minutes for two hours while these mixtures were exposed to direct sunlight, covering a wavelength range of 350 to 530 nm. Furthermore, 1 mL of 0.2 M NaBH₄ was added to the AgNP solutions at concentrations of 4000 ppm and 267 ppm, including MO, in order to evaluate the impact of a reducing agent. Absorbance was then measured for the same wavelength range using DW as the blank [33].

PNP degradation by AgNPs

10 ppm PNP and 600 ppm NaBH₄ aqueous solutions were prepared. There were three phases involved in the catalytic reduction of PNP by all five varieties of synthesized AgNPs. The absorbance of PNP was measured first from 280 to 500 nm using DW as the blank. This was followed by measurement of absorbance from 280 to 500 nm for 1 mL of PNP and 2 mL of NaBH₄ mixture and 1 mL of PNP, 2 mL of NaBH₄, and 20 µL of AgNP mixture. DW was used as the blank, and the absorbance was measured every 5 minutes for a 30-minute time period [34].

Antibacterial activity of AgNPs and WEs

Muller-Hinton's (MH) agar was prepared and autoclaved at 121°C for 15 minutes. Into labeled sterile petri plates (Fig. 2), cooled MH agar was poured and let to solidify. Subcultured *E. coli* and *S. aureus* were introduced into separated test tubes containing 0.9% saline using an inoculation loop and mixed. The turbidity was maintained at 0.5% of the McFarland standard. 1 ml of each WE and AgNP was dried in the dry oven at 60°C for 20 minutes. On the solidified petri plates, respective bacterial inoculums were streaked using a cotton swab. Wells were created on S1, S2, and negative regions using sterilized pipette tips. Samples were added to their respective wells. Gentamicin served as the positive control for the assay, while 0.9% saline served as the negative control. The plates were incubated for 24 hours at 34°C, and the ZOI was determined.

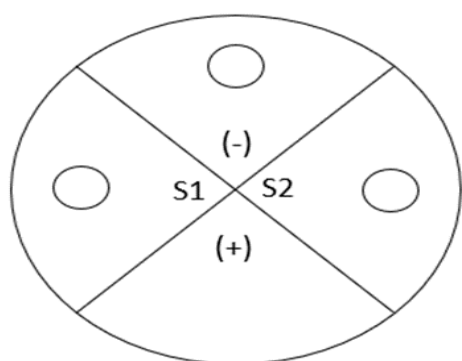


Fig. 2 Labeling of petri plate: (+) Gentamycin, (-) Saline, (S1) Sample 01, (S2) Sample 02.

Cytotoxic assessment

Filtered saltwater obtained from Mount Lavinia Beach, Sri Lanka, was used to grow the brine shrimp eggs for 24 hours using an aerator and yellow lamp. Using seawater, two AgNP dilutions with concentrations of 800 ppm and 240 ppm were prepared. On a 96-well plate, 200 µL of each AgNP dilution and two brine shrimps

were added in triplicates. A control was also performed with seawater and two brine shrimps. After a 24-hour incubation period under a yellow light, the percentage viability of each AgNP dilution was determined [35].

RESULTS

Characterization of *Zinnia elegans* leaf AgNP

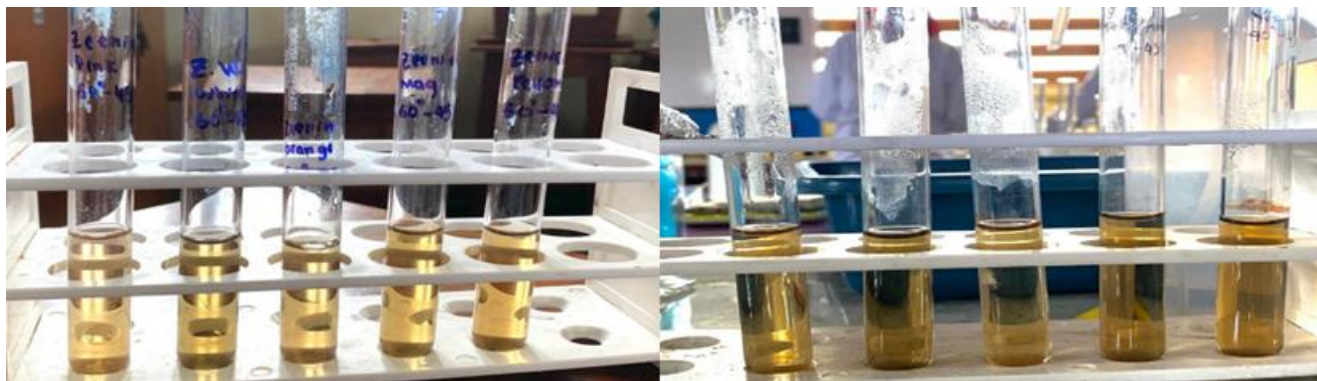


Fig. 3 A distinctive colour shift from pale yellow (A) to dark yellow (B) confirming the formation of AgNPs.

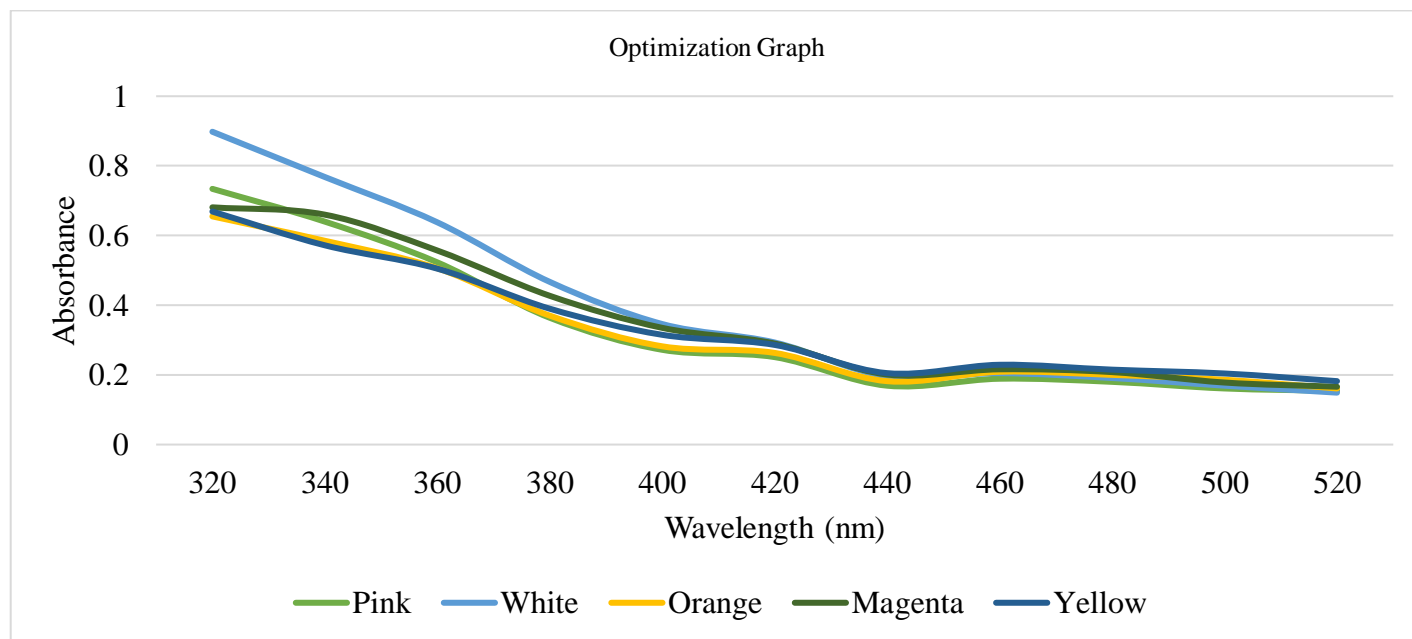


Fig. 4 UV-visible spectrum of AgNPs synthesised using five different varieties of *Z. elegans* leaf at 90°C for 45 minutes.

Table 1. Optimization table

Temp	Time	Pink	White	Orange	Magenta	Yellow
90°C	60mins	✗	✗	✗	✗	✗
	45mins	✓	✓	✓	✓	✓
	30mins	✗	✗	✓	✗	✗
	15mins	✗	✗	✗	✗	✗
60°C	60mins	✗	✗	✗	✗	✗
	45mins	✗	✗	✗	✗	✗
	30mins	✗	✗	✗	✗	✗
	15mins	✗	✗	✗	✗	✗
RT	24hrs	✗	✗	✗	✓	✗

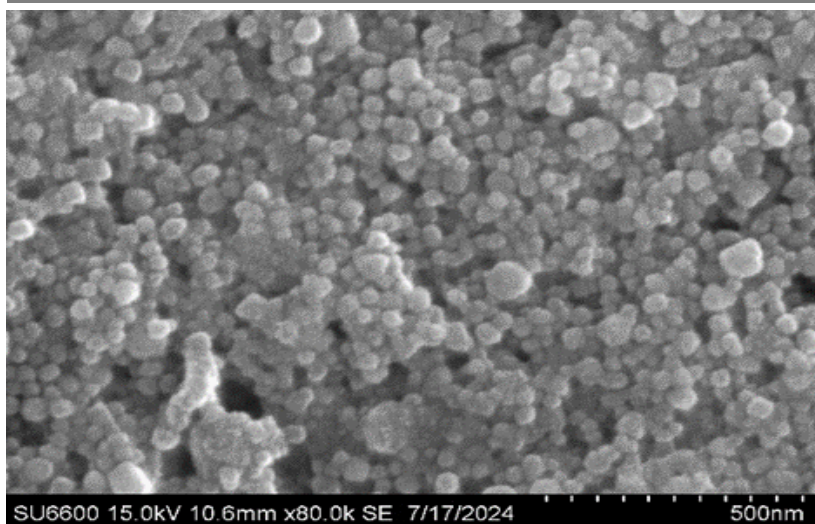


Fig. 5 SEM analysis of Magenta_AgNP at 15kV 10.6 mm ×80.0k- 500 nm

Photocatalytic degradation of *Zinnia elegans* leaf AgNP.

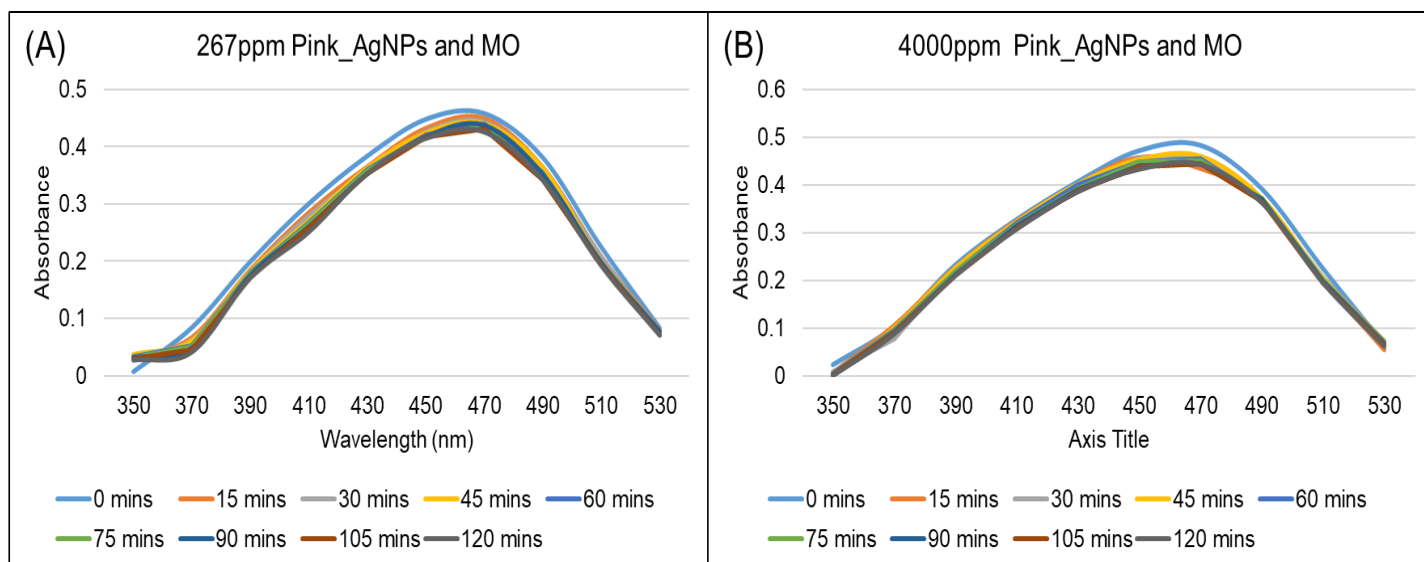


Fig. 6 Degradation of 1 ppm MO dye using 1 mL of Pink_AgNP under various conditions: (A) 267 ppm in the presence of sunlight, (B) 4000 ppm in the presence of sunlight.

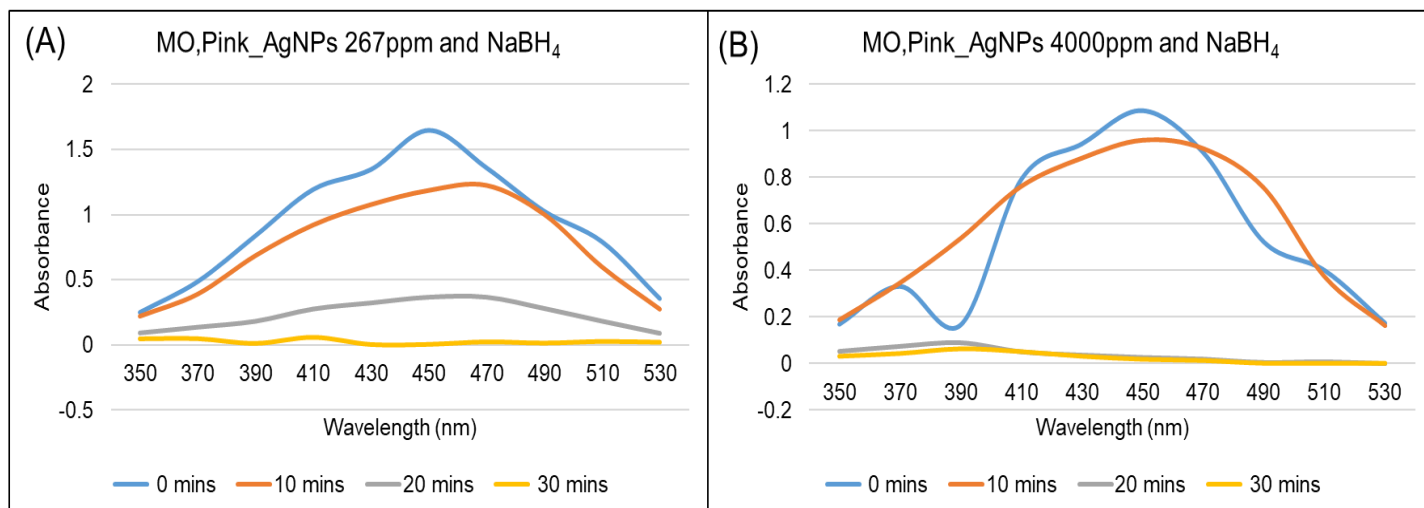


Fig. 7 Degradation of 1 ppm MO dye using 1 mL of Pink_AgNP under various conditions (A) 267 ppm in the presence of sunlight and 0.2 M NaBH₄, (B) 4000 ppm in the presence of sunlight and 0.2 M NaBH₄.

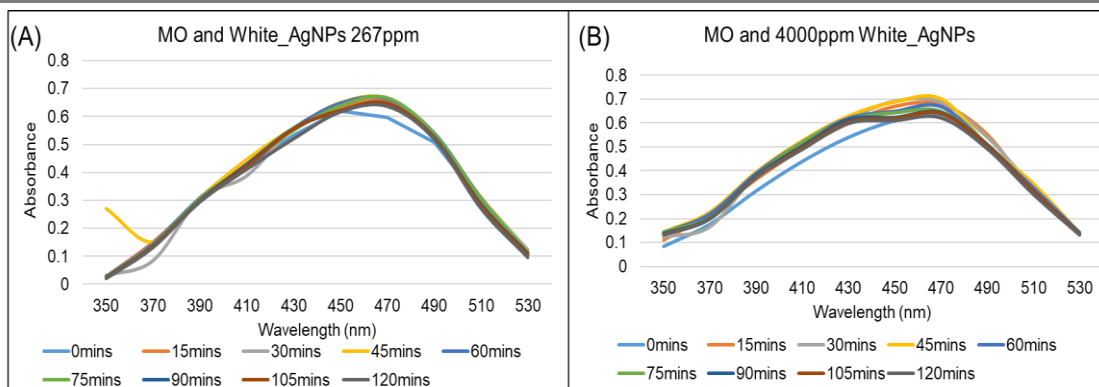


Fig. 8 Degradation of 1 ppm MO dye using 1 mL White_AgNP under various conditions: (A) 267 ppm in the presence of sunlight, (B) 4000 ppm in the presence of sunlight.

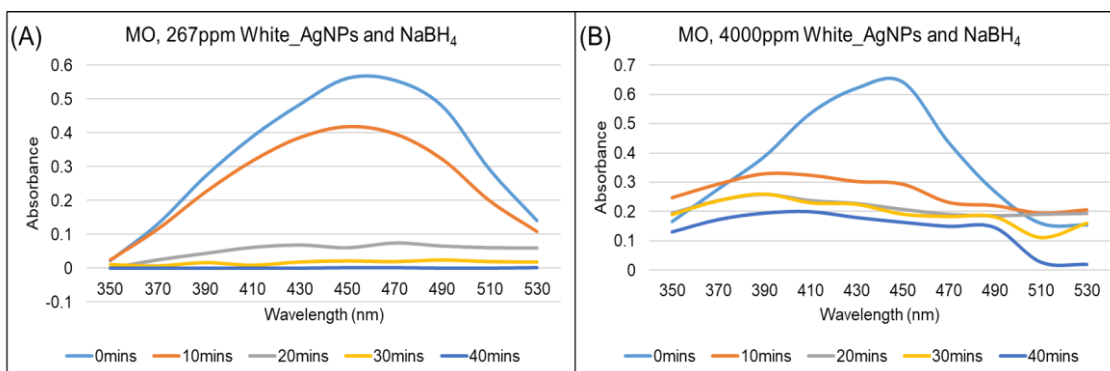


Fig. 9 Degradation of 1 ppm MO dye using 1 mL White_AgNP under various conditions: (A) 267 ppm in the presence of sunlight and 0.2 M NaBH₄, (B) 4000 ppm in the presence of sunlight and 0.2 M NaBH₄.

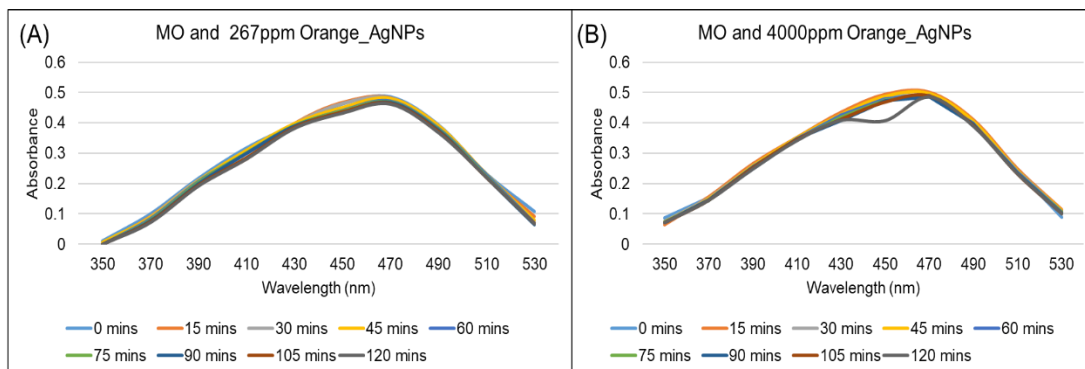


Fig. 10 Degradation of 1 ppm MO dye using 1 mL Orange_AgNP under various conditions: (A) 267 ppm in the presence of sunlight, (B) 4000 ppm in the presence of sunlight.

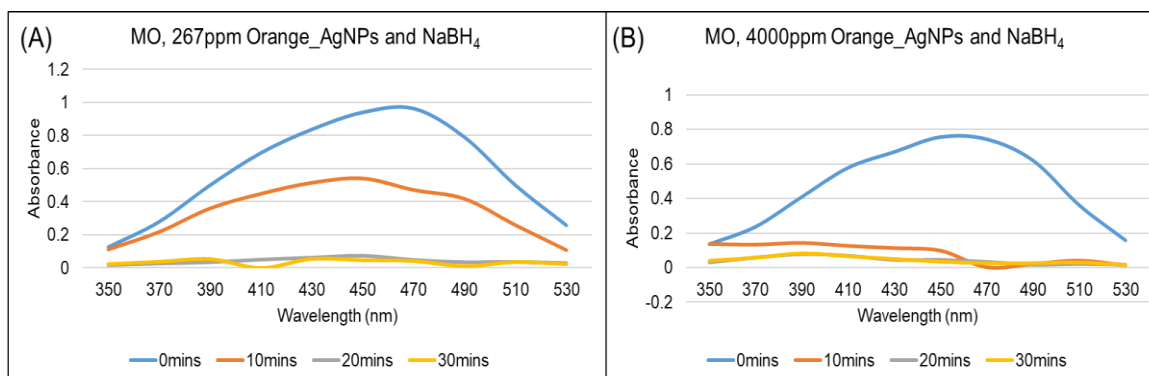


Fig. 11 Degradation of 1 ppm MO dye using 1 mL Orange_AgNP under various conditions: (A) 267 ppm in the presence of sunlight and 0.2 M NaBH₄, (B) 4000 ppm in the presence of sunlight and 0.2 M NaBH₄.

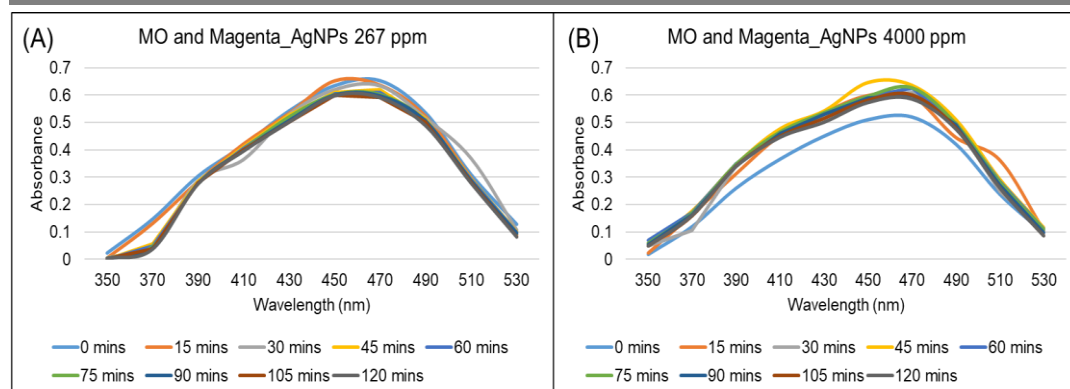


Fig. 12 Degradation of 1 ppm MO dye using 1 mL Magenta_AgNP under various conditions: (A) 267 ppm in the presence of sunlight, (B) 4000 ppm in the presence of sunlight.

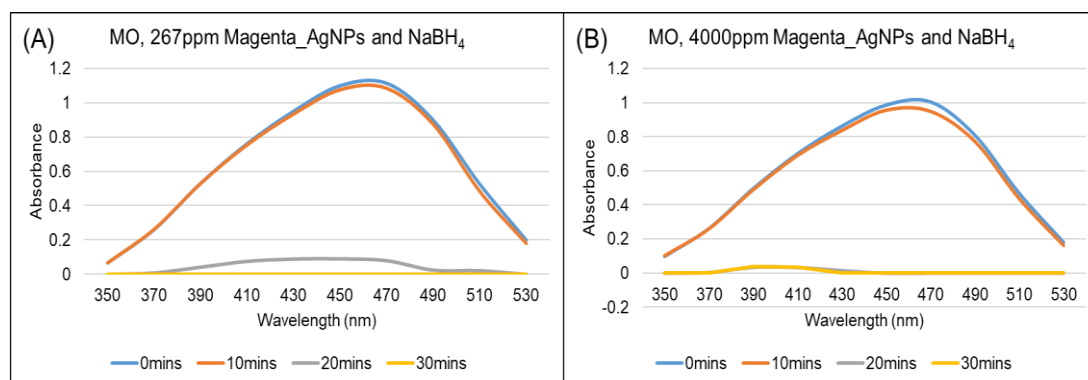


Fig. 13 Degradation of 1 ppm MO dye using 1 mL Magenta_AgNP under various conditions: (A) 267 ppm in the presence of sunlight and 0.2 M NaBH₄, and (B) 4000 ppm in the presence of sunlight and 0.2 M NaBH₄.

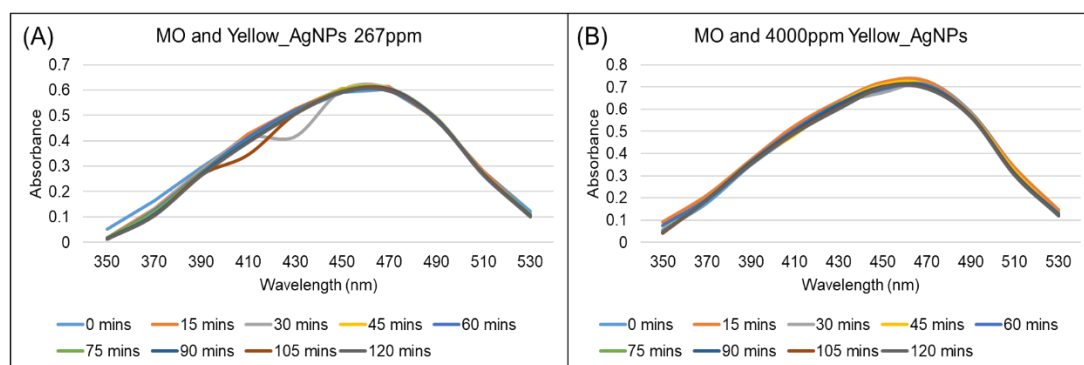


Fig. 14 Degradation of 1 ppm MO dye using 1 mL Magenta_AgNP under various conditions: (A) 267 ppm in the presence of sunlight, (B) 4000 ppm in the presence of sunlight

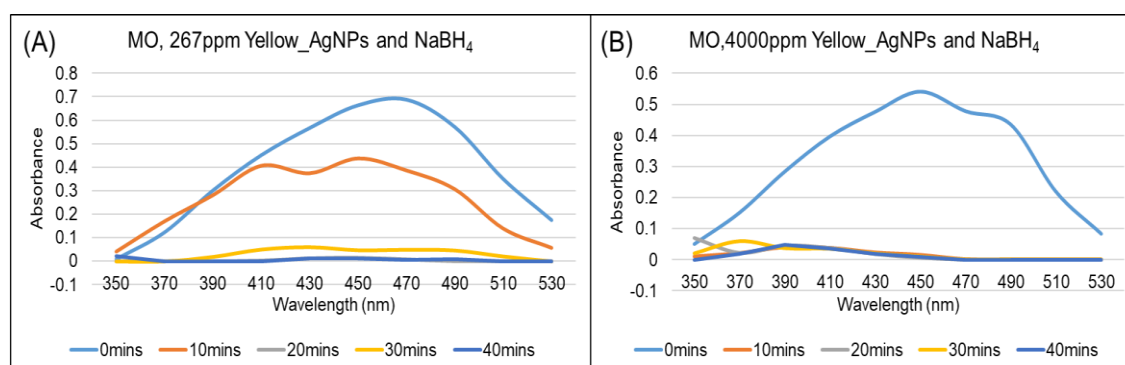


Fig. 15 Degradation of 1 ppm MO dye using 1 mL Magenta_AgNP under various conditions: (A) 267 ppm in the presence of sunlight and 0.2 M NaBH₄, (B) 4000 ppm in the presence of sunlight and 0.2 M NaBH₄.

PNP degradation of *Zinnia elegans* leaf AgNP.

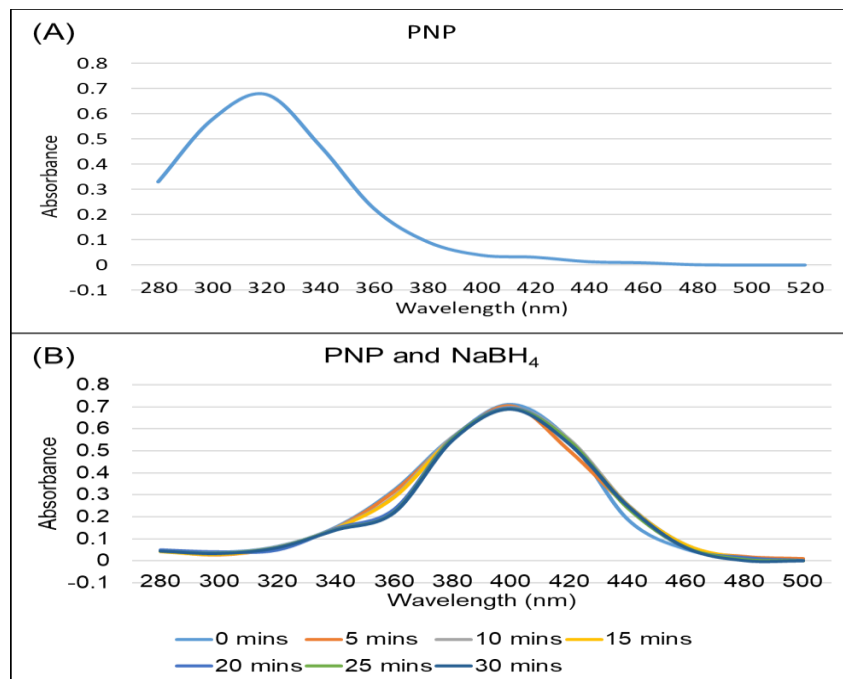


Fig. 16 Peak shift in UV-visible absorption spectra: (A) 1 mL of 10 ppm PNP and (B) 1 mL of 10 ppm PNP and 600 ppm NaBH₄

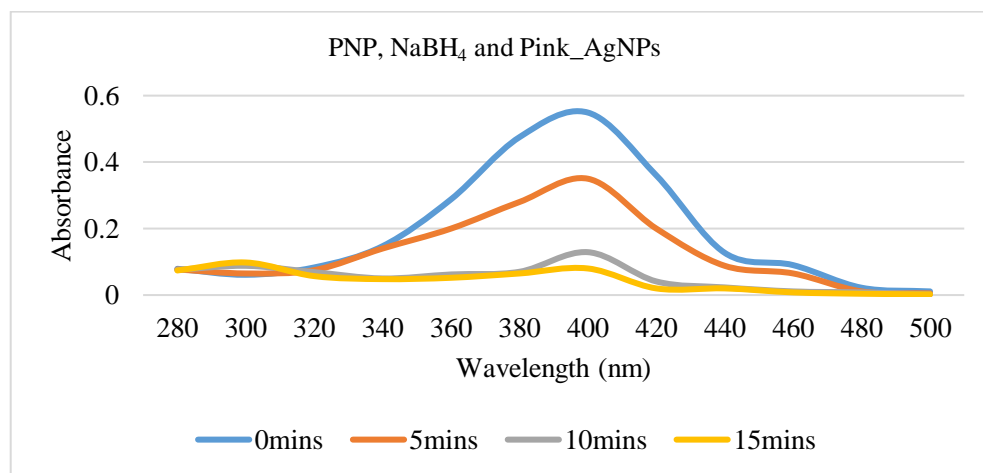


Fig. 17 PNP degradation with 20 μ L of 4000 ppm Pink_AgNP and 600 ppm NaBH₄.

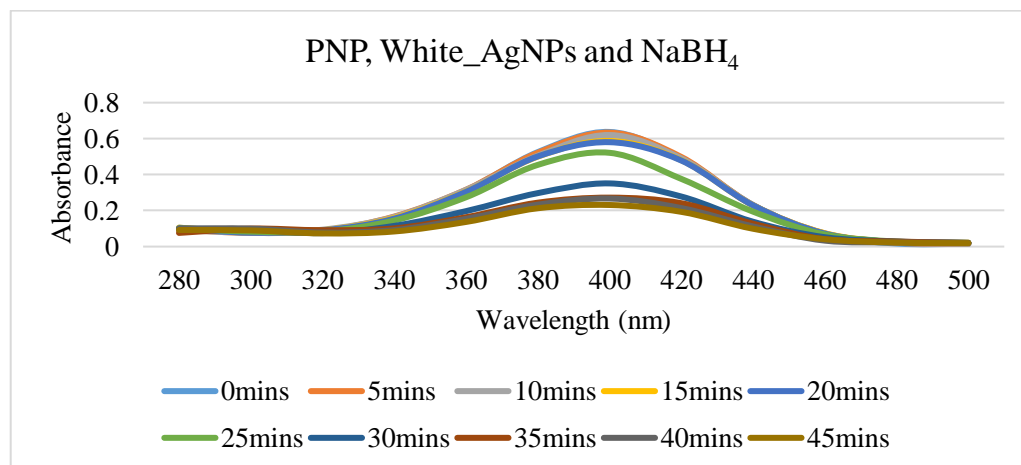


Fig. 18 PNP degradation with 20 μ L of 4000 ppm White_AgNP and 600 ppm NaBH₄.

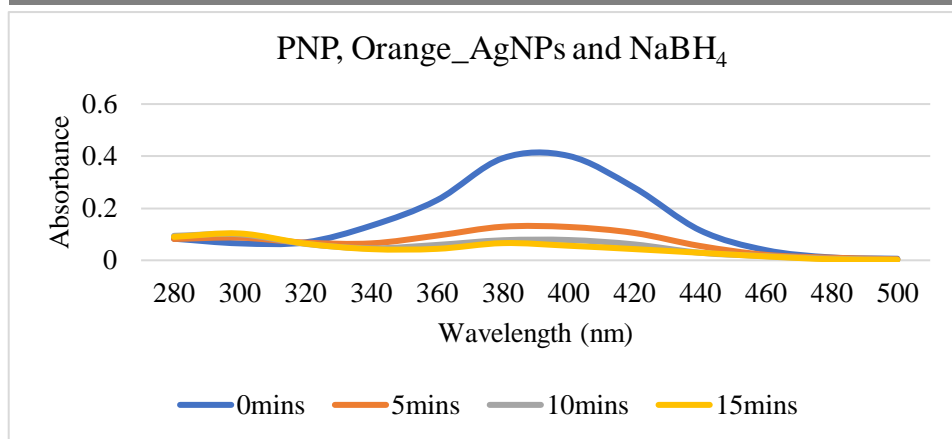


Fig. 19 PNP degradation with 20 µl of 4000 ppm Orange_AgNP and 600 ppm NaBH₄.

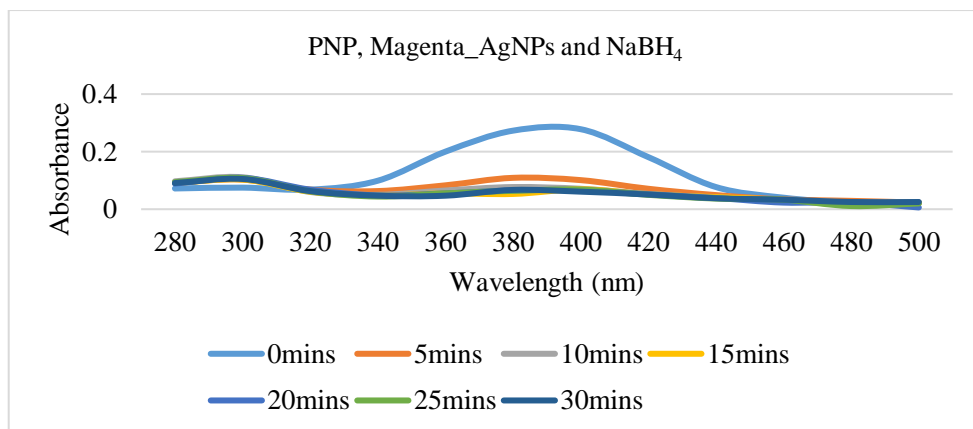


Fig. 20 PNP degradation with 20 µl of 4000 ppm Magenta_AgNP and 600 ppm NaBH₄.

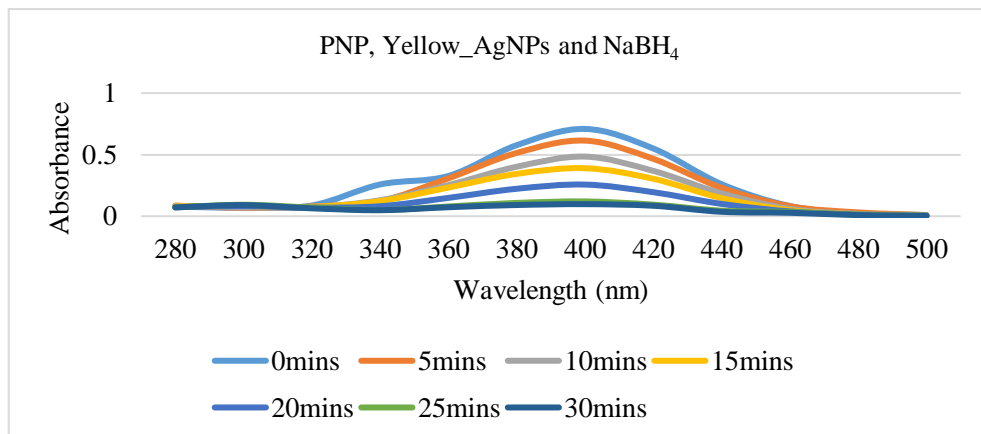


Fig. 21 PNP degradation with 20 µl of 4000 ppm Yellow_AgNP and 600 ppm NaBH₄.

Antibacterial activity of *Zinnia elegans* leaf AgNP

Table II. ZOI for *E.coli* using WE and AgNP

Sample	S1 / (cm)	S2 / (cm)	Average / (cm)	Positive Control / (cm)
Pink_WE	-	-	-	3.6
White_WE	-	-	-	3.5
Orange_WE	-	-	-	3.5
Magenta_WE	-	-	-	3.3
Yellow_WE	-	-	-	3.5
Pink_AgNPs	1.6	1.5	1.6	3.5

White_AgNPs	1.5	1.5	1.5	2.8
Orange_AgNPs	1.5	1.5	1.5	3.3
Magenta_AgNPs	1.2	1.4	1.3	3.0
Yellow_AgNPs	2.0	1.5	1.8	3.0

Table III. ZOI for *S.aureus* using WE and AgNP

Sample	S1/ (cm)	S2/ (cm)	Average/ (cm)	Positive Control/ (cm)
Pink_WE	-	-	-	3.8
White_WE	-	-	-	3.8
Orange_WE	-	-	-	4.0
Magenta_WE	-	-	-	4.0
Yellow_WE	-	-	-	4.0
Pink_AgNPs	1.2	1.3	1.3	3.8
White_AgNPs	1.2	1.4	1.3	4.0
Orange_AgNPs	1.5	1.3	1.4	4.0
Magenta_AgNPs	1.3	1.4	1.4	3.8
Yellow_AgNPs	1.5	1.3	1.4	3.7

DISCUSSION

Green synthesis and characterization of *Zinnia elegans* leaf AgNP.

Phytochemicals such as flavonoids, alkaloids, phenolic acids, and saponins are bioactive compounds that are naturally present in plants and provide protection from environmental stressors [36]. Studies also confirm the presence of the saponins, tannins, flavonoids, phenols, and quinones as phytochemicals along with triterpenoids and diterpenoids in *Zinnia* leaves [37]. These phytochemicals act as bioactive components necessary in the AgNP synthesis procedure. In green synthesis, bioactive compounds present in plant extracts reduce Ag^+ ions to Ag^0 [38]. Following the formation of Ag atoms, agglomeration takes place to form the nanoparticle. The stabilization of this structure is achieved by bonding of the functional groups of bioactive compounds with the metallic salt [39]. The factors that influence the synthesis of AgNPs include physiochemical parameters such as temperature, pH, and concentration of salts and reducing agents [40].

Detecting the presence of AgNP is crucial after its effective synthesis. Following the incubation period, a color shift and an absorbance peak are observed. A phenomenon called the surface plasmon resonance (SPR) effect is responsible for these observations. The SPR effect occurs when light causes electrons on the surface of the nanoparticles to oscillate, absorbing particular light wavelengths. Color variations brought on by this phenomenon can be detected using spectrophotometry. A peak between 400 and 480 nm and a characteristic color shift from dark brown to reddish brown are indicators of the presence of AgNPs [41,42].

In this study, the impact of two physiochemical parameters—temperature and time—was assessed. *Zinnia* leaf AgNP synthesis was subjected to varying temperatures and durations. All samples of *Zinnia* leaves synthesized AgNPs only at 90°C for 45 minutes (Table I) with a color change from light yellow to dark yellow (Fig. 3). AgNP synthesis was also confirmed as a peak was observed at 460 nm for all five samples (Fig. 4). However, previous studies conducted on *Zinnia elegans* Jacq. showed maximum absorbance peak at 439 nm, *Sanvitalia procumbens* which is a plant belonging to the Asteraceae family reported similar peak; 438 nm with 0.01 mol/L AgNO_3 solution, *Zinnia* leaf AgNP from ethanol extract and 250 μL of 10^{-2} M AgNO_3 showed peaks at 410 to 420 nm range [43 – 45].

It has been demonstrated that the nucleation process is aided by exposure to high temperatures during AgNP synthesis because of the accelerated rate of reaction. On the other hand, high temperatures cause AgNP to reduce in size [46]. The synthesis process is also influenced by the reaction time; longer incubation times result in increased AgNPs. According to prior research, 40 minutes is the ideal duration because all of the nanonuclei have fully developed into agglomerated nanoparticles [47]. In this study, 90°C for 45 minutes only showed the presence of AgNP, further proving the previously documented findings. A study on *Arctium lappa* and

Eupatorium odartum leaf which belong to the same family as *Zinnia* showed AgNP synthesis at 90°C [48, 49]. Similar research using *Vernonia amygdalina*, a member of the Asteraceae family, has also reported the observed color change. This study claims that the characteristic color change is caused by the addition of DW rather than methanol or ethanol [50].

SEM analysis was conducted to characterize the size and shape of the AgNPs. Magenta_AgNP were in the size range of 30-60 nm and were spherical (Fig. 5). Size and shape of AgNPs are vital factors that influence their functional properties. The uniform nature of the shape observed suggests a controlled synthesis [51]. Previous studies showed that AgNPs synthesized by samples of the same family but different species were of similar nature [43, 52]. This outcome is one of the factors that contributed to the results of the activities that were tested.

Applications of *Zinnia elegans* leaf AgNP

Zinnia elegans belonging to the Asteraceae family plants which is a family reported to have various different applications such as photocatalytic activity, anti-cancer activity, anti-diabetic and anti-microbial activity [53].

Photocatalytic degradation of *Zinnia elegans* leaf AgNP

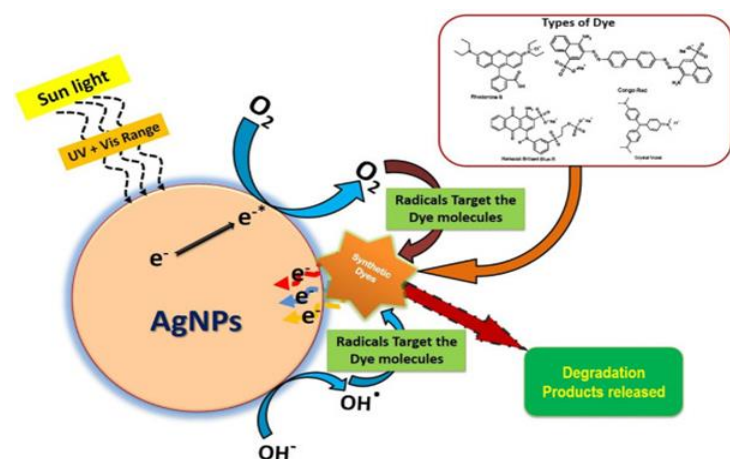


Fig. 22 AgNP photocatalytic mechanism of action [44].

The photocatalytic effect of AgNPs was evaluated using MO dye. The mechanism of action involves the generation of reactive species that can degrade organic contaminants. AgNPs can absorb light, which excites electrons, creating electron-hole pairs. Such pairs produce reactive species such as superoxide, hydrogen peroxide, and hydroxyl radicals, which facilitate the degradation of organic contaminants by breaking down the azo bonds (Fig. 22). The above process contains a high kinetic energy barrier, making degradation a slow process without the use of any additional agents [55]. The presence of NaBH_4 , which acts as a reducing agent, facilitates the transfer of electrons to the reactive species that allow an efficient degradation of organic dyes. The high surface area of AgNP makes it easier for BH_4^- and dye molecules to be absorbed onto the surface and thereby facilitates the electron transfer from BH_4^- to the dye molecule [56, 57].

In this study, the degradation of MO under sunlight was assessed in which results indicate that the degradation was very slow and showcased limited photocatalytic activity (Fig. 6,8,10, 12 and 14). However, upon the addition of NaBH_4 , a significant increase in the rate of degradation of MO was observed (Fig. 7, 9, 11, 13 and 15).

Magenta_AgNP showed complete degradation within 10 minutes for 4000 ppm and within 20 minutes for 267 ppm (Fig. 15). The kinetics of MO degradation by AgNP in the presence of sunlight and NaBH_4 was conducted. A first-order reaction was applied according to the equation $\ln (c_t/c_0) = -kt$, where c_0 and c_t represent the absorbance value of dye at each time interval and at the initial state, and k is the rate constant [58]. The rate constant (k) was obtained by plotting $\ln (c_t/c_0)$ against the reaction time t as shown in Fig. 23 and 24.

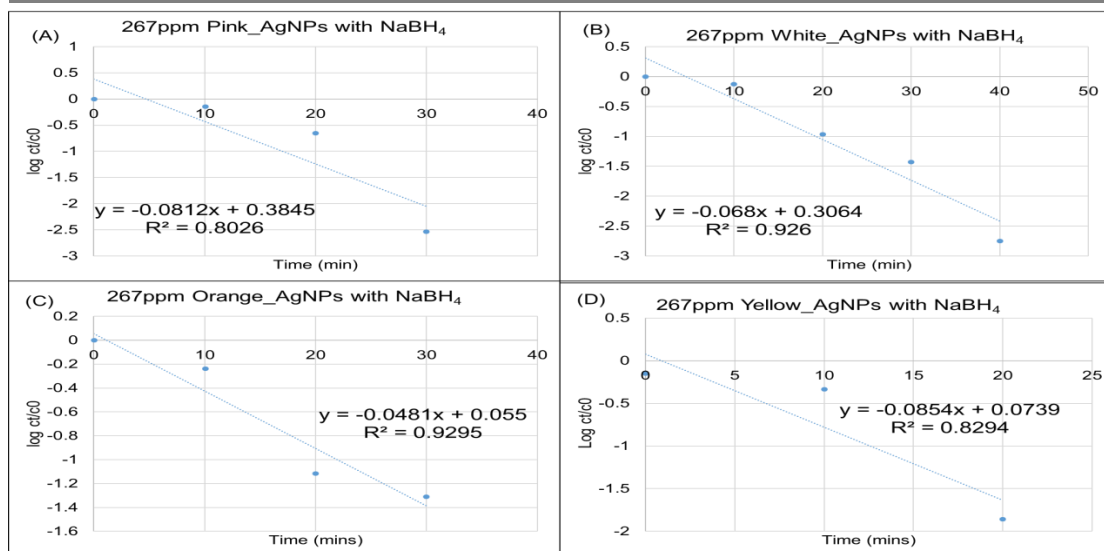


Fig. 23 MO dye degradation kinetics in the presence of sunlight and NaBH₄ at (A) 266 ppm Pink_AgNP, (B) 266 ppm White_AgNP, (C) 266 ppm Orange_AgNP, (D) 266 ppm Magenta_AgNP and (E) 266 ppm Yellow_AgNP

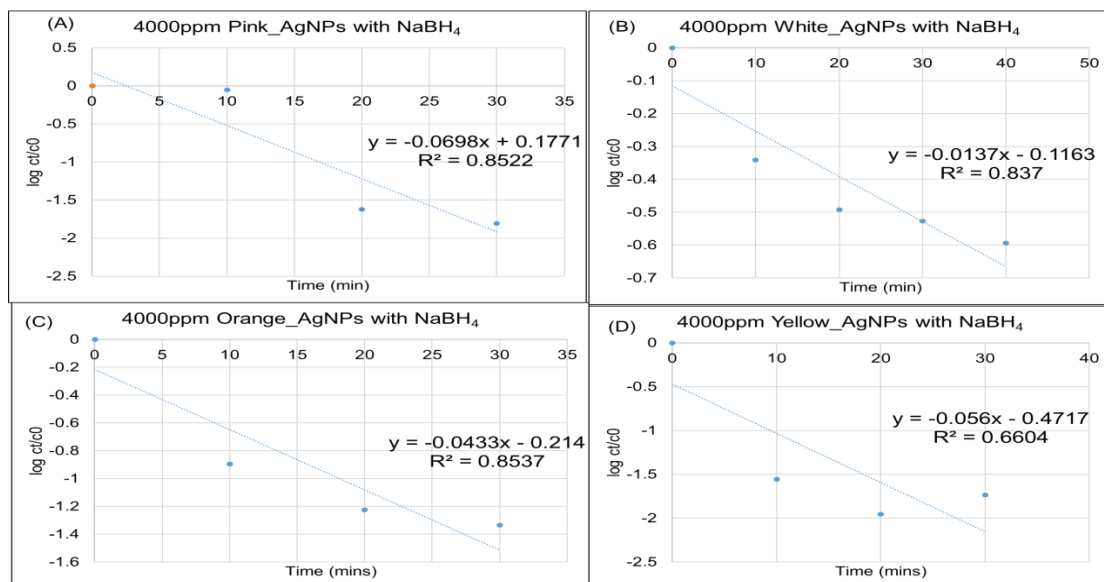


Fig. 24 MO dye degradation kinetics in the presence of sunlight and NaBH₄ at ((A) 4000 ppm Pink_AgNP, (B) 4000 ppm White_AgNP, (C) 4000 ppm Orange_AgNP, (D) 4000 ppm Magenta_AgNP and (E) 4000 ppm Yellow_AgNP Table IV. MO degradation rate constants of the synthesized *Zinnia* leaf AgNPs in the presence of sunlight and NaBH₄

Sample ID	267 ppm	4000 ppm
Pink_AgNP	0.0812	0.0698
White_AgNP	0.068	0.0137
Orange_AgNP	0.0481	0.0433
Yellow_AgNP	0.0854	0.056

From the rate constants calculated, the 267 ppm samples showed the highest rate of degradation compared to 4000 ppm. The lowest rate was observed in White_AgNP at 4000 ppm (Table IV). This suggests that low concentration of *Zinnia elegans* leaf AgNP is required for the complete degradation of MO. Previous research reported successful degradation of MO by AgNPs synthesized by a species of the same family, hence supporting the results obtained in this study [59]. Researches support plants belonging to the family Asteraceae as good photocatalytic nanoparticles; this study was focused on the degradation of Orange G dye with 15 ppm *S. procumbens* AgNP and Direct Blue-15 Azo Dye with *S. procumbens* 10 ppm showing about 70%

degradation of both dyes by 180 minutes [43]. Similar study using *Ageratum conyzoides* L. leaf AgNP for the degradation of MB showed 100% degradation by 105 minutes with a rate of $2.8 \times 10^{-2} \text{ min}^{-1}$ [60].

PNP degradation of *Zinnia elegans* leaf AgNP.

The catalytic degradation of PNP using AgNPs was conducted to assess the effectiveness of AgNPs in breaking down organic contaminants. PNP can be degraded using NaBH_4 , which acts as a reducing agent and donates electrons to PNP to convert it to less toxic compound; 4-aminophenol (PAP). The production of p-nitrophenolate ions in the solution causes a shift in the absorbance peak from 317 nm to 400 nm and the color change from light yellow to deep yellow [61]. However, this possesses a high activation energy, making it non-feasible to react without the presence of a catalyst [62]. AgNPs act as a catalyst and a site for the reaction to occur. In the presence of AgNPs, the electrons from NaBH_4 reduce PNP to PAP. AgNPs aid in facilitating the electron transfer process by lowering the activation energy. In the presence of AgNP, the absorbance peak at 400 nm significantly decreases, indicating the breakdown of PNP, and the absorbance peak at 300 nm increases as a result of PAP formation [63, 64].

Results obtained in this study showed a shift in the peak in the addition of NaBH_4 with no significant degradation with time (Fig. 16). However, upon the addition of AgNPs, which act as a catalyst in this reaction, degradation was observed (Fig. 17-21), demonstrating the effectiveness of *Zinnia* AgNPs as catalysts and their potential in this application. The kinetics was calculated by applying first-order kinetics according to the equation $\ln c_t/c_0 = -kt$, where c_t and c_0 are the absorbance of 4-nitrophenolate ion at the reaction time t and zero. The rate constant (k) was determined (Fig. 25), and the highest degradation rate was determined.

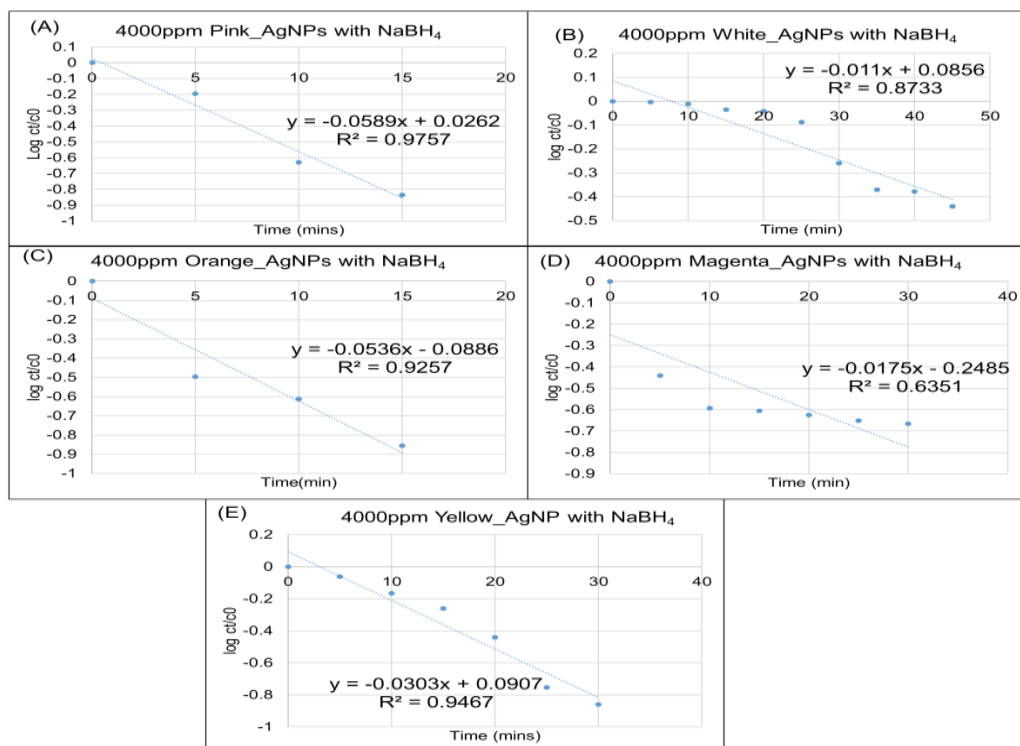


Fig. 25 Kinetics of PNP degradation with 600 ppm NaBH_4 at (A) 4000 ppm Pink_AgNP, (B) 4000 ppm White_AgNP, (C) 4000 ppm Orange_AgNP, (D) 4000 ppm Magenta_AgNP and (E) 4000 ppm Yellow_AgNP

Table V: Summary of Rate constants for PNP degradation

Sample ID	Rate constants
Pink_AgNP	0.0589
White_AgNP	0.011
Orange_AgNP	0.0536
Magenta_AgNP	0.0175
Yellow_AgNP	0.0303

The highest rate of degradation can be observed in Pink_AgNP whilst the lowest can be observed in White_AgNP (Table V). However, there is no supporting evidence for these findings since this experiment has not yet been performed on *Zinnia* AgNPs. A similar research was conducted using *Saussurea obvallata* AgNPs which belongs to the Asteraceae family. There was no degradation even after 24 hour incubation of PNP and NaBH₄. The addition of 5 mg and 10 mg of AgNP showed successful degradation of PNP by 24 minutes and 14 minutes respectively. The reported rates of degradation of 5 mg and 10 mg AgNP was 0.1477 and 0.1596 respectively [65].

Antibacterial activity of *Zinnia elegans* leaf AgNP

The antibacterial assessment of AgNPs and WEs was conducted by measuring the ZOI against *E. coli* and *S. aureus*. The mechanism of action of AgNP against bacterial strains is classified into two pathways: action at the membrane level of the bacteria and alterations in the cellular content of bacteria. AgNP has the ability to bind to the bacterial cell membrane, causing damage, increased permeability of the membrane, and finally cell death due to leakage of cellular matter. AgNP is reported to have the ability to directly influence the cellular mechanisms within the bacteria by altering the structure and the function of DNA and proteins within the bacteria (Fig. 26) [66].

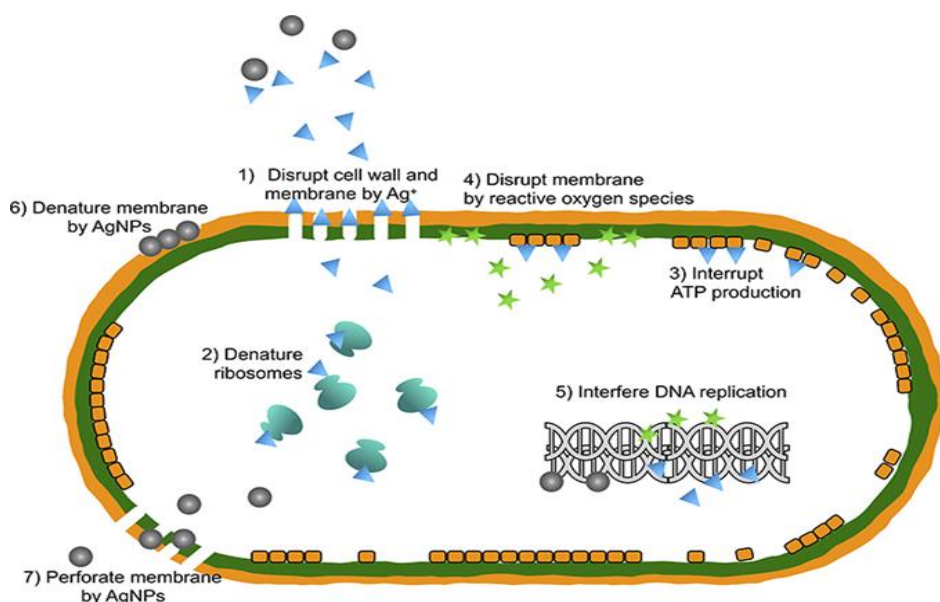


Fig. 26 Antibacterial effect of AgNPs [55].

All five AgNP samples exhibit ZOIs displaying antibacterial activity; however, WEs showed no significant ZOIs, indicating a lack of antibacterial activity (Tables II and III). The findings of this experiment also indicate that *Zinnia* AgNPs have a higher efficiency against *E. coli* (Table II). This is caused by the thin cell wall in gram-negative bacterial strains compared to gram-positive strains. This further demonstrates how crucial AgNP uptake by bacterial strains is to the antibacterial activity [68, 69]. The previous research performed with the AgNPs synthesized from *Calendula officinalis* L, *Carthamus tinctorius*, *Eupatorium odoratum* and *Tagetes erecta* which are species of the same family reported high antibacterial effects against *E. coli* and *S. aureus*, hence supporting the results of this study [49, 70 – 72]. Using ciprofloxacin as the antibiotic, another study on the antibacterial effect on *E. coli* and *S. aureus* produced similar findings: higher activity against gram-negative strains was reported at pH 5, and higher activity against gram-positive strains was observed at pH 7 [73].

Cytotoxicity activity of *Zinnia elegans* leaf AgNP

The cytotoxic assessment was conducted on the synthesized AgNPs using *Artemia salina*. The frequent utilization of AgNP as an alternative in different industries makes it essential to evaluate the toxicity it poses. The features AgNPs demonstrate in antibacterial activity can also influence eukaryotic cells which can lead to DNA damage and cell cycle arrest [74, 75].

In this study, brine shrimps were exposed to two different AgNP concentrations of 800 ppm and 240 ppm, and viability rate was recorded after 24 hours. The mechanism of AgNP cytotoxicity involves the generation of ROS, cell membrane disruption, and interaction with cellular components affecting metabolic reactions (Fig. 27) [76].

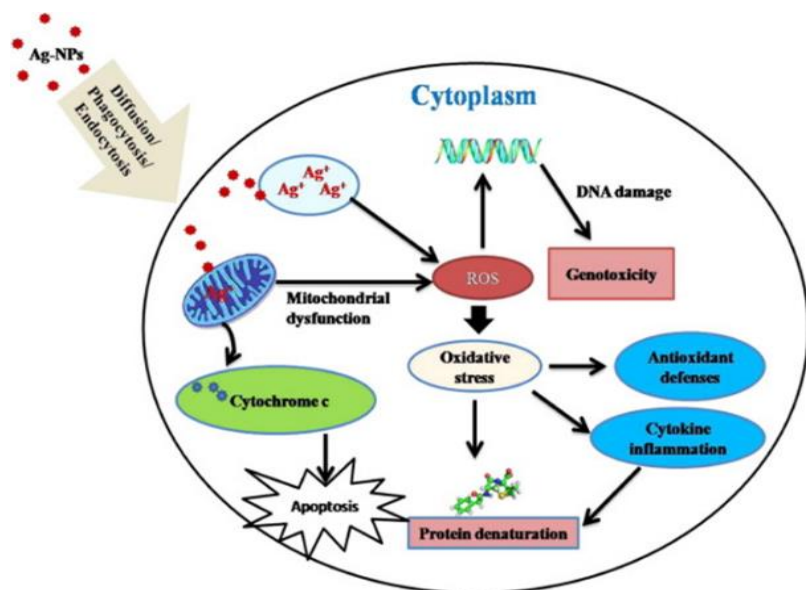


Fig. 27 Cytotoxic effect of AgNPs [63].

The presence of AgNP aggregates in the gut is the morphological alteration that brine shrimps exhibit following AgNP incubation. Brine shrimps have a non-filter feeding technique that allows them to ingest any particle below the size of 50 microns. The concentration of AgNPs to which brine shrimp are exposed and the quantity of AgNPs they ingest will determine how the shrimp are affected by AgNPs [33].

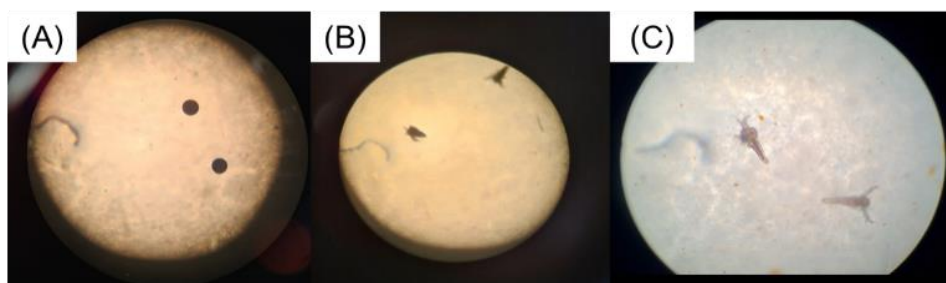


Fig. 28 Different stages of *Artemia salina* morphology: (A) eggs, (B) hatchlings prior to AgNP incubation, and (C) following AgNP incubation.

The obtained results indicate a 100% viability of both tested concentrations for all five synthesized AgNPs (Fig. 28), indicating that the synthesized AgNPs do not contain any cytotoxic effect and are safe for use. This could be due to the lower AgNP size showcased by the synthesized AgNPs. The results of a previous research also indicate that AgNPs produced by a species of the same family also showed a low cytotoxic effect [78]. A research using *Zinnia elegans* leaf AgNP reported higher cytotoxicity against cancer cells compared to endothelial cells and another study reported cytotoxicity against cancer cells by *Artemisia marschalliana* and *A. turcomanica* AgNPs which belong to the same family as *Zinnia* [45,53].

CONCLUSION

In conclusion, WEs from five different *Zinnia* leaf varieties—Pink, White, Orange, Magenta, and Yellow—synthesized AgNPs at 90°C for 45 minutes, showing a characteristic dark yellow color change and absorbance peak at 460 nm. The SEM analysis of Magenta_AgNP showed spherical AgNPs in the range of 30 to 60 nm. The photocatalytic degradation study of 4000 ppm and 266 ppm AgNPs demonstrated an increased rate of reaction with the addition of NaBH₄. The highest rate was observed in 4000 ppm AgNPs. Among the five

AgNPs that demonstrated catalytic efficiency in the PNP degradation study, Pink_AgNP exhibited the highest rate of reaction. The antibacterial evaluation revealed ZOI for AgNPs against *S. aureus* and *E. coli*. All five varieties of AgNP show higher efficiency against *E. coli*. Additionally, the cytotoxic evaluation showed 100% viability at 800 ppm and 240 ppm AgNP, demonstrating biocompatibility and safety. Based on these findings, *Zinnia* leaf AgNPs can be regarded as harmless substances that will be helpful in antibacterial and bioremediation treatments.

ACKNOWLEDGMENT

The authors are acknowledging the support provided by Northumbria University, UK in PNP catalysis and Institute of Nanotechnology (SLINTEC), Sri Lanka for allowing usage of the Hitachi SU6600 for SEM analysis.

REFERENCES

1. Masure P. S. & Patil B. M. (2014). "Extraction of Waste Flowers", International Journal of Engineering Research & Technology (IJERT). DOI: 10.17577/IJERTV3IS110067
2. Dutta, S. & Kumar, M.S. (2021). "Potential of value-added chemicals extracted from floral waste: A review". Journal of Cleaner Production. DOI: <https://doi.org/10.1016/j.jclepro.2021.126280>
3. Srivastav, A.L. & Kumar, A. (2021). "An endeavor to achieve sustainable development goals through floral waste management: A short review" Journal of Cleaner Production. DOI: <https://doi.org/10.1016/j.jclepro.2020.124669>
4. Gomaa, A., et al. (2019). "A comprehensive review of phytoconstituents and biological activities of genus *Zinnia*". Journal of advanced Biomedical and Pharmaceutical Sciences. DOI: 10.21608/jabps.2018.5599.1024
5. Bessada, S.M.F., et al. (2015). "Asteraceae species with most prominent bioactivity and their potential applications: A review." Industrial Crops and Products. DOI: <https://doi.org/10.1016/j.indcrop.2015.07.073>.
6. Burlec, A.F., et al. (2019). "Chemical Profile and Antioxidant Activity of *Zinnia elegans* Jacq. Fractions." Molecules. DOI: 10.3390/molecules24162934.
7. Mohamed, A.H., et al. (2015). "Hepatoprotective and Antioxidant Activity of *Zinnia Elegans* Leaves Ethanolic Extract." International Journal of Scientific & Engineering Research.
8. Guo, D., et al. (2013). "Mechanical properties of nanoparticles: basics and applications." Journal of Physics D: Applied Physics. DOI: <https://doi.org/10.1088/0022-3727/47/1/013001>.
9. Yusuf, M. (2019). "Silver Nanoparticles: Synthesis and Applications." Handbook of Ecomaterials. DOI: https://doi.org/10.1007/978-3-319-68255-6_16.
10. Iravani, S., et al. (2014). "Synthesis of silver nanoparticles: chemical, physical and biological methods." Research in Pharmaceutical Sciences
11. Ritu, et al. (2023). "Phytochemical-Based Synthesis of Silver Nanoparticle: Mechanism and Potential Applications." BioNano Science. DOI: <https://doi.org/10.1007/s12668-023-01125-x>.
12. Ravindran, et al. (2013). "Biofunctionalized silver nanoparticles: Advances and prospects." Colloids and Surfaces B: Biointerfaces. DOI: <https://doi.org/10.1016/j.colsurfb.2012.07.036>.
13. Bhakya, S., et al. (2015). "Catalytic Degradation of Organic Dyes using Synthesized Silver Nanoparticles: A Green Approach." Journal of Bioremediation & Biodegradation. DOI: 10.4172/2155-6199.1000312
14. Al-Tohamy, R., et al. (2022). "A critical review on the treatment of dye-containing wastewater: Ecotoxicological and health concerns of textile dyes and possible remediation approaches for environmental safety." Ecotoxicology and Environmental Safety. DOI: <https://doi.org/10.1016/j.ecoenv.2021.113160>
15. Benkhaya, S., et al. (2020). "Classifications, properties, recent synthesis and applications of azo dyes." Heliyon. DOI: <https://doi.org/10.1016/j.heliyon.2020.e03271>
16. Hanafi, M.F. & Sapawe, N. (2020). "A review on the water problem associate with organic pollutants derived from phenol, methyl orange, and remazol brilliant blue dyes." Materials Today: Proceedings. DOI: <https://doi.org/10.1016/j.matpr.2021.01.258>

17. Jiku, M.A.S., et al. (2021). "Toxic wastewater status for irrigation usage at Gazipur and Savar industrial vicinity of Bangladesh." *Acta Ecol. Sin.* DOI: <https://doi.org/10.1016/j.chnaes.2021.07.001>
18. Ao, S. & Zayed T. (2022). "Impact of sewer overflow on public health: a comprehensive scientometric analysis and systematic review." *Environ. Res.* DOI: <https://doi.org/10.1016/j.envres.2021.111609>
19. Anandan, S., et al. (2020). "A review on hybrid techniques for the degradation of organic pollutants in aqueous environment." *Ultrasonics Sonochemistry*. DOI: <https://doi.org/10.1016/j.ultsonch.2020.105130>.
20. Samuel, M.S., et al. (2020). "Biosynthesized silver nanoparticles using *Bacillus amyloliquefaciens*; Application for cytotoxicity effect on A549 cell line and photocatalytic degradation of p-nitrophenol." *Journal of Photochemistry and Photobiology B: Biology*. DOI: <https://doi.org/10.1016/j.jphotobiol.2019.111642>.
21. Wu, H., et al. (2023). "N-doped carbon nanoflakes coordinate with amorphous Fe to activate ozone for degradation of p-nitrophenol." *Colloids and surfaces. A, Physicochemical and engineering aspects*. DOI: <https://doi.org/10.1016/j.colsurfa.2023.132173>.
22. Frieri, M., et al. 2017. "Antibiotic resistance." *Journal of Infection and Public Health*. DOI: <https://doi.org/10.1016/j.jiph.2016.08.007>.
23. Mirzajani, F., et al. (2011). "Antibacterial effect of silver nanoparticles on *Staphylococcus aureus*." *Research in Microbiology*. DOI: <https://doi.org/10.1016/j.resmic.2011.04.009>.
24. Al-Sa'ady, A., et al. (2020). "Antibacterial activities of chlorine gas and chlorine dioxide gas against some pathogenic bacteria." *EurAsian Journal of BioSciences Eurasia J Biosci.*
25. Liao, C., et al. (2019). "Bactericidal and Cytotoxic Properties of Silver Nanoparticles." *International Journal of Molecular Sciences*. DOI: <https://doi.org/10.3390/ijms20020449>
26. Slavin, Y.N., et al. (2017). "Metal nanoparticles: understanding the mechanisms behind antibacterial activity." *J Nanobiotechnol*. DOI: <https://doi.org/10.1186/s12951-017-0308-z>
27. Dakal, T.C, et al. (2016). "Mechanistic Basis of Antimicrobial Actions of Silver Nanoparticles." *Front. Microbiol.* DOI: [10.3389/fmicb.2016.01831](https://doi.org/10.3389/fmicb.2016.01831)
28. Tripathi, N. & Goshisht, M.K. (2022). "Recent Advances and Mechanistic Insights into Antibacterial Activity, Antibiofilm Activity, and Cytotoxicity of Silver Nanoparticles." *ACS Applied Bio Materials*. DOI: <https://doi.org/10.1021/acsabm.2c00014>.
29. Fröhlich, E.E & Fröhlich, E. (2016). "Cytotoxicity of Nanoparticles Contained in Food on Intestinal Cells and the Gut Microbiota." *International Journal of Molecular Sciences*. DOI: <https://doi.org/10.3390/ijms17040509>
30. Chernousova, S. & Eppe, M. (2012). "Silver as Antibacterial Agent: Ion, Nanoparticle, and Metal." *Angewandte Chemie International Edition*. DOI: <https://doi.org/10.1002/anie.201205923>
31. Morais, M., et al. (2020). "Cytotoxic Effect of Silver Nanoparticles Synthesized by Green Methods in Cancer." *Journal of Medicinal Chemistry*. DOI: <https://doi.org/10.1021/acs.jmedchem.0c01055>.
32. Morejón, B., et al. (2018). "Larvicidal Activity of Silver Nanoparticles Synthesized Using Extracts of *Ambrosia arborescens* (Asteraceae) to Control *Aedes aegypti* L. (Diptera: Culicidae)." *Journal of Nanotechnology*. DOI: <https://doi.org/10.1155/2018/6917938>.
33. Latha, D., et al. (2017). "Photocatalytic Activity of Biosynthesized Silver Nanoparticle from Leaf Extract of *Justicia Adhatoda*. Mechanics," *Materials Science & Engineering Journal*. DOI: <https://doi.org/10.2412/mmse.81.72.41>.
34. Mahiuddin, M., et al. (2020). "Green Synthesis and Catalytic Activity of Silver Nanoparticles Based on *Piper chaba* Stem Extracts." *Nanomaterials*. DOI: <https://doi.org/10.3390/nano10091777>
35. Arulvasu, C., et al. (2014). "Toxicity Effect of Silver Nanoparticles in Brine Shrimp *Artemia*." *The Scientific World Journal*. DOI: [10.1155/2014/256919](https://doi.org/10.1155/2014/256919)
36. Johnson, I.T. (2007). "Phytochemicals and cancer." *Proceedings of the Nutrition Society*. DOI: <https://doi.org/10.1017/s0029665107005459>.
37. Samy, M.N., et al. (2022). "Flavonoids of *Zinnia elegans*: Chemical profile and, in vitro antioxidant and in silico anti-COVID-19 activities." *South African Journal of Botany*. DOI: <https://doi.org/10.1016/j.sajb.2022.02.024>.
38. Bedlovičová, Z., et al. (2020). "A Brief Overview on Antioxidant Activity Determination of Silver Nanoparticles." *Molecules*. DOI: <https://doi.org/10.3390/molecules25143191>.

39. Jabeen, S., et al. (2021). "Application of green synthesized silver nanoparticles in cancer treatment—a critical review." *Mater. Res. Express*. DOI: 10.1088/2053-1591/ac1de3
40. Ulaeto, S. B., et al. (2019). "Biogenic Ag nanoparticles from neem extract: their structural evaluation and antimicrobial effects against *Pseudomonas nitroreducens* and *Aspergillus unguis* (NII 08123)." *ACS Biomater Sci Eng*. DOI: <https://doi.org/10.1021/acsbiomaterials.9b01257>
41. Asif, M., et al. (2022). "Green Synthesis of Silver Nanoparticles (AgNPs), Structural Characterization, and their Antibacterial Potential." *Dose Response*. DOI: 10.1177/15593258221088709.
42. Jiang, Z., et al. (2012). "The surface-plasmon-resonance effect of nanogold/silver and its analytical applications." *Trends in Analytical Chemistry*. DOI: <https://doi.org/10.1016/j.trac.2012.03.015>.
43. Aslam, M., et al., (2021). "Phyto-Extract-Mediated Synthesis of Silver Nanoparticles Using Aqueous Extract of *Sanvitalia procumbens*, and Characterization, Optimization and Photocatalytic Degradation of Azo Dyes Orange G and Direct Blue-15." *Molecules*. DOI: 10.3390/molecules26206144
44. Singh, Y., et al., (2021). "Phytotoxic assessment of AgNO₃ and ZnSO₄ vis à vis AgNPs and ZnONPs in *Tagetes erecta* L. and *Zinnia elegans* Jacq." *Plant Archives*. DOI: <https://doi.org/10.51470/PLANTARCHIVES.2021.v21.S1.109>
45. Haque, S., et al., (2021). "Biosynthesized Silver Nanoparticles for Cancer Therapy and In Vivo Bioimaging." *Cancers (Basel)*. DOI: 10.3390/cancers13236114
46. Liu, H., et al. (2017). "Effect of temperature on the size of biosynthesized silver nanoparticle: Deep insight into microscopic kinetics analysis." *Arabian Journal of Chemistry*. DOI:10.1016/j.arabjc.2017.09.004
47. Hong, G.B, et al. (2022). "Facile Synthesis of Silver Nanoparticles and Preparation of Conductive Ink." *Nanomaterials (Basel)*. DOI: 10.3390/nano12010171.
48. Nguyen, T.TN., et al. (2018). "Silver and gold nanoparticles biosynthesized by aqueous extract of burdock root, *Arctium lappa* as antimicrobial agent and catalyst for degradation of pollutants." *Environ Sci Pollut Res*. DOI: <https://doi.org/10.1007/s11356-018-3322-2>
49. Elemike, E. E., et al., (2017). "Green Synthesis of Ag/Ag₂O Nanoparticles Using Aqueous Leaf Extract of *Eupatorium odoratum* and Its Antimicrobial and Mosquito Larvicidal Activities." *Molecules*. DOI: <https://doi.org/10.3390/molecules22050674>
50. Kumavat, S.R. & Mishra, S. (2021). "Green synthesis of silver nanoparticles using *Borago officinalis* leaves extract and screening its antimicrobial and antifungal activity." *Int Nano Lett* . DOI: <https://doi.org/10.1007/s40089-021-00345-x>
51. Mukherji, S., et al. (2018). "Synthesis and characterization of size- and shape-controlled silver nanoparticles." *Physical Sciences Reviews*. DOI: <https://doi.org/10.1515/psr-2017-0082>.
52. Tüzün, B.S., et al. (2018). "Green bio-inspired synthesis, characterization and activity of silver nanoparticle forms of *Centaurea virgata* Lam. and the isolated flavonoid eupatorin." *Green Processing and Synthesis*. DOI:<https://doi.org/10.1515/gps-2017-0027>.
53. Jaison, J. P., et al., (2023). "Green Synthesis of Bioinspired Nanoparticles Mediated from Plant Extracts of Asteraceae Family for Potential Biological Applications." *Antibiotics*. DOI: <https://doi.org/10.3390/antibiotics12030543>
54. Marimuthu, S., et al. (2020). "Silver nanoparticles in dye effluent treatment: A review on synthesis, treatment methods, mechanisms, photocatalytic degradation, toxic effects and mitigation of toxicity." *Journal of Photochemistry and Photobiology B: Biology*. DOI: <https://doi.org/10.1016/j.jphotobiol.2020.111823>.
55. Katta, V.K.M. & Dubey, R.S. (2020). "Green synthesis of silver nanoparticles using *Tagetes erecta* plant and investigation of their structural, optical, chemical and morphological properties." *Materials Today: Proceedings*. DOI: <https://doi.org/10.1016/j.matpr.2020.02.809>.
56. Jara, Y.S, et al. (2024). "Highly efficient catalytic degradation of organic dyes using iron nanoparticles synthesized with *Vernonia Amygdalina* leaf extract." *Sci Rep*. DOI: 10.1038/s41598-024-57554-5.
57. Ghosh, B. K., et al. (2015). "Preparation of Cu nanoparticle loaded SBA-15 and their excellent catalytic activity in reduction of variety of dyes." *Powder Technol*. DOI: <https://doi.org/10.1016/j.powtec.2014.09.027>
58. Paul, S.C., et al. (2020). "Silver Nanoparticles Synthesis in a Green Approach: Size Dependent Catalytic Degradation of Cationic and Anionic Dyes." *Orient J Chem*. DOI : <http://dx.doi.org/10.13005/ojc/360301>

59. Rajasekar, R., et al. (2022). "Ecofriendly synthesis of silver nanoparticles using *Heterotheca subaxillaris* flower and its catalytic performance on reduction of methyl orange." *Biochemical Engineering Journal*. DOI:<https://doi.org/10.1016/j.bej.2022.108447>.
60. Chandraker, S.K., et al., (2019). "DNA-binding, antioxidant, H₂O₂ sensing and photocatalytic properties of biogenic silver nanoparticles using *Ageratum conyzoides* L. leaf extract." *RSC Advance*. DOI: 10.1039/C9RA03590G.
61. Sudhakar, P. & Soni, H. (2018). "Catalytic reduction of nitrophenols using silver nanoparticles-supported activated carbon derived from agro-waste." *J. Environ. Chem. Eng.* DOI: <https://doi.org/10.1016/j.jece.2017.11.053>
62. Shimoga, G., et al. (2020). "Catalytic Degradability of p-Nitrophenol Using Ecofriendly Silver Nanoparticles." *Metals*. DOI:<https://doi.org/10.3390/met10121661>.
63. Erdem, H.B. & Çetinkaya, S. (2022). "Facile insitu preparation of silver nanoparticles supported on petroleum asphaltene-derived porous carbon for efficient reduction of nitrophenols." *Heliyon*. DOI: <https://doi.org/10.1016/j.heliyon.2022.e10659>
64. Shah, Z., et al. (2021). "Synthesis of high surface area AgNPs from *Dodonaea viscosa* plant for the removal of pathogenic microbes and persistent organic pollutants." *Materials Science and Engineering: B*. DOI:<https://doi.org/10.1016/j.mseb.2020.114770>.
65. Sagar, P.S.R. V., Ramadevi, D., Basavaiah, K. and Botsa, S.M. 2024. Green synthesis of silver nanoparticles using aqueous leaf extract of *Saussurea obvallata* for efficient catalytic reduction of nitrophenol, antioxidant, and antibacterial activity. *Water Science and Engineering*, 17 (3), pp. 274-282. DOI: <https://doi.org/10.1016/j.wse.2023.09.004>.
66. Bruna, T., et al. (2021). "Silver Nanoparticles and Their Antibacterial Applications." *Int J Mol Sci*. DOI: 10.3390/ijms22137202.
67. Yin, I.X., et al. (2020). "The Antibacterial Mechanism of Silver Nanoparticles and Its Application in Dentistry." *International Journal of Nanomedicine*. DOI:<https://doi.org/10.2147/ijn.s246764>.
68. Meikle, T., et al. (2020). "Preparation, characterization, and antimicrobial activity of cubosome encapsulated metal nanocrystals." *ACS Appl Mater Interfaces*. DOI: 10.1021/acsami.9b21783
69. Mai-Prochnow, A., et al. (2016). "Gram positive and Gram negative bacteria differ in their sensitivity to cold plasma." *Sci Rep*. DOI: <https://doi.org/10.1038/srep38610>
70. Rodríguez-Felix, F., et al., (2021). "Sustainable-green synthesis of silver nanoparticles using safflower (*Carthamus tinctorius* L.) waste extract and its antibacterial activity." *Heliyon*. DOI: 10.1016/j.heliyon.2021.e06923
71. Maji, A., et al., (2020). "Study on the antibacterial activity and interaction with human serum albumin of *Tagetes erecta* inspired biogenic silver nanoparticles." *Process Biochemistry*. DOI :10.1016/j.procbio.2020.07.017
72. Ghanati, F. & Bakhtiarian, S. (2014). "Effect of methyl jasmonate and silver nanoparticles on production of secondary metabolites by *Calendula officinalis* L (Asteraceae)." *Tropical Journal of Pharmaceutical Research*. DOI:<https://doi.org/10.4314/tjpr.v13i11.2>.
73. Tesfaye, M., et al. (2023). "Green synthesis of silver nanoparticles using *Vernonia amygdalina* plant extract and its antimicrobial activities," *Heliyon*. DOI: <https://doi.org/10.1016/j.heliyon.2023.e17356>
74. Verkhovskii, R., et al. (2019). "Physical properties and cytotoxicity of silver nanoparticles under different polymeric stabilizers," *Heliyon*. DOI: <https://doi.org/10.1016/j.heliyon.2019.e01305>
75. AshaRani, P. V., et al. (2009). "Cytotoxicity and genotoxicity of silver nanoparticles in human cells." *ACS nano*. DOI: <https://doi.org/10.1021/nn800596w>
76. Pinheiro, K. de P., et al. (2020). "Toxic effects of silver nanoparticles on the germination and root development of lettuce (*Lactuca sativa*)." *Australian Journal of Botany*. DOI: <https://doi.org/10.1071/bt19170>.
77. Akter, M., et al. (2018). "A systematic review on silver nanoparticles-induced cytotoxicity: Physicochemical properties and perspectives," *Journal of Advanced Research*. DOI: <https://doi.org/10.1016/j.jare.2017.10.008>.
78. Jamil, K., et al. (2022). "Biogenic Synthesis of Silver Nanoparticles Using *Catharanthus roseus* and Its Cytotoxicity Effect on Vero Cell Lines." *Molecules*. DOI: <https://doi.org/10.3390/molecules27196191>.